JOURNAL OF Materials CHEMISTRY

Synthesis and characterization of a polystyrene sulfonate layered double hydroxide nanocomposite. *In-situ* polymerization *vs.* polymer incorporation†

El Mostafa Moujahid, Jean-Pierre Besse and Fabrice Leroux*

Laboratoire des Matériaux Inorganiques, UMR 6002, Université Blaise Pascal, 63177 Aubière cédex, France. E-mail: fleroux@chimtp.univ-bpclermont.fr

Received 17th June 2002, Accepted 24th June 2002
First published as an Advance Article on the web 3rd October 2002

Vinyl benzene sulfonate (styrene sulfonate — VBS) and polystyrene sulfonate (PSS) are incorporated into layered double hydroxides (LDH) of nominal composition $Zn_nAl(OH)_{2(1+n)}Cl{\cdot}nH_2O$ by exchange and *templating* reaction, respectively. PSS adsorption leads to a delamination process of the LDH 2D-host structure. A hydrothermal treatment improves greatly the crystallinity of the PSS–LDH nanocomposite. The interactions between VBS and the host structure are evaluated by ^{13}C CP-MAS solid state NMR spectroscopy. The electrostatic binding between the sulfonate group and the inner-surface of the LDH host structure causes some shifts in the resonance lines, although the shifts are independent of the LDH layer charge density. *In-situ* polymerization of VBS molecules between LDH sheets is reached after soft heat treatment. Its completion requires a good matching between the layer charge density and the projected surface area of the guest molecule as exemplified by a Zn to Al ratio of 2. In comparison to the pristine material, the change from *Oh* to *Td* aluminium site is substantially reduced for PSS–LDH nanocomposite and absent for the material prepared after the polymerization reaction.

Introduction

For the past decade, nanocomposites built from an assembly of a lamellar inorganic host structure and a polymer have attracted considerable interest.[1–4] Owing to the highly tunable properties, they may find applications in a large number of fields such as those emphasizing mechanical enhancement, gas permeability or polymer electrolytes.[5–8]

We focused our attention on the system composed of polystyrene sulfonate (PSS) as the guest polymer and a layered double hydroxide (LDH). The inorganic solids influence the PSS flammability properties.[9,10]

The materials of nominal composition $Zn_nAl(OH)_{2(1+n)}Cl{\cdot}nH_2O$, noted as Cl-[$Zn_nAl$], were chosen as the inorganic host framework. Lamellar LDH structure is commonly described as edge-sharing octahedra sheets in which, by comparison with the brucite $M(OH)_2$, some of the divalent cations are replaced by trivalent cations.[11,12] The excess of charge, *i.e.* Al^{3+} content, is counter-balanced by interlayered anions, leading to an anionic exchange capacity (AEC). The latter may be as high as 2.46 meq g^{-1} and associated with a layer charge density of 25.4 $Å^2$ per e^- for a ratio *n* Zn to Al of 2. Such characteristics are inconvenient for the intercalation/diffusion of large molecules such as polymers.[13]

To overcome this issue, and as illustrated in the literature, the incorporation of polymers between an inorganic host structure may be achieved by the *in-situ* polymerization of a monomer, or the encapsulation of the polymer *via* restacking of the inorganic layers or *via* the *templating* method.

In-situ polymerization was used for the incorporation of polyaniline (PANI) into various host structures, such as V_2O_5,[14] $HNbMoO_6$,[15] FeOCl,[16] α-$RuCl_3$,[17] MoO_3,[18] and graphitic oxide.[19] The other two methods consist of a transformation of the host material into a colloid–suspension system and precipitation in the presence of the polymer. The polymer is incorporated during the crystal growth, the so-called *templating* method,[20,21] or after exfoliation of the layers.[22,23] The latter is not appropriate for the restacking of large molecules from [Zn_nAl] LDH layers.[4] The former method gives rise to ill-defined polymer–LDH nanocomposites,[20,24] as usually observed for other systems.[25]

In the present contribution, a curing post-treatment is used for PSS–[Zn_2Al] LDH nanocomposites obtained *via* the *templating* method. Earlier work has shown the possibility of obtaining a PSS–LDH nanocomposite,[24] although, the material was ill-defined. To our knowledge, the *in-situ* polymerization has never been reported. The solids are characterized by X-ray diffraction and absorption techniques. The interaction of the VBS monomer with the inner-surface of the LDH material is analyzed by ^{13}C solid state NMR spectroscopy. *In-situ* polymerization is mostly limited by two factors:[4] the monomer to monomer distance when present in the interlamellar space, and the conditions for the polymerization (temperature, pH or redox reaction), which must leave the layered structure intact. The *in-situ* polymerization of VBS is studied as a function of the temperature and of the LDH layer charge density.

Experimental section

Incorporation of the organic moiety

The starting materials Cl-[Zn_nAl] (n = 2, 3 and 4) were prepared by coprecipitation as described by Miyata[26] from solutions of $ZnCl_2$ (98%, Aldrich) and $AlCl_3$ (99%, Aldrich). A 250 ml solution containing Al and Zn of total cation concentration of 10^{-2} M was prepared, with Zn to Al ratio following *n*. The synthesis is performed under flowing N_2 gas to avoid any contact with atmospheric CO_2. The solution was added dropwise into 250 ml decarbonated water under vigorous stirring, at a constant pH value depending on *n* (pH = 8.3, 7.9 and 7.5 for n = 2, 3, and 4, respectively). The addition of NaOH (1 M) was completed after 24 hours. The suspension was aged in the mother liquor during stirring for

†Basis of a presentation given at Materials Discussion No. 5, 22–25 September 2002, Madrid, Spain.

 DOI: 10.1039/b205837p

24 hours. The white solid products were isolated by repeated centrifuging and washing with decarbonated water and were finally dried at room temperature.

The same procedure was used for the preparation of Cl-[Mg_2Al], with pH fixed at 10.5.

The amount of sodium styrene-4-sulfonate, $CHCH_2C_6H_4SO_3Na$ (Fluka, >90%) corresponded to twice the anionic exchange capacity (AEC) of the LDH sample. The solution was stirred for 72 hours under nitrogen atmosphere. The solids were separated as previously described. Similar conditions were employed for the intercalation of dodecylbenzene sulfonate (Na-DBS, $CH_3(CH_2)_{11}C_6H_4SO_3Na$, Fluka, >95%).

PSS–LDH nanocomposites were prepared by the *templating* method described by Lerner *et al.*[20] Sodium polystyrene-4-sulfonate (Acros, M_w of 70 000) used without further purification was dissolved in aqueous media. A solution containing $ZnCl_2$ and $AlCl_3{\cdot}6H_2O$ is added dropwise to the previous one. The conditions were similar to the synthesis performed in the absence of polymer.

In-situ polymerization and post-synthesis procedures

VBS–LDH hybrid materials were treated at different temperatures in air or nitrogen atmosphere for 4 hours. The colour of the samples turns from white to yellow. In order to improve the crystallinity, a hydrothermal treatment was carried out for PSS–LDH samples. They were placed in a sealed Teflon® tube, and kept at 120 °C for two days under autogenous pressure.

Elemental analysis (H, C, S, Al and Zn) was performed at the Vernaison Analysis Center of CNRS using inductive conduction plasma coupled to atomic emission spectroscopy (ICP/AES). The chemical compositions are reported in Table 1.

Technique of characterization

X'Pert Pro Philips equipped with a HTK16 Anton Paar chamber and a PSD-50 m Braun detector was used to record XRD diagrams. The conditions were: step width of 0.0387°, time per step of 60 s, an aperture on 2° (155 channels).

^{13}C (I = 1/2) and ^{27}Al (I = 5/2) solid state NMR experiments were performed with a 300 Bruker spectrometer at 75.47 and 78.20 MHz, respectively. For both nuclei, the experiments were carried out using magic angle spinning (MAS) conditions at 10 kHz and a 4 mm diameter size zirconia rotor. ^{13}C spectra obtained by proton enhanced cross-polarization method (CP) are referenced to the carbonyl of the glycine calibrated at 176.03 ppm.

For ^{27}Al nuclei, $Al(H_2O)_6^{3+}$ was used as a reference. Short radio frequency pulses associated with a recycling time of 500 ms were used. Chemical shifts are not corrected from the second order quadrupolar effect which induces a shift to lower frequency.[27]

Zn k-edge: EXAFS (*extended X-ray absorption fine structure*) studies were performed at LURE (Orsay, France) using X-ray synchrotron radiation emitted by the DCI storage ring (1.85 GeV positrons, average intensity of 250 mA) at the D44 line. Data were collected at room temperature in transmission mode at the Zn k-edge (9 658.6 eV). A double-crystal Si (111) monochromator scanned the energy in 2 eV steps from 100 eV below to 900 eV above the Zn k absorption edge, three spectra were recorded for each sample. The accumulation time was 2 s per point. After extraction by standard procedures,[28] the EXAFS spectra were evaluated by the classical plane-wave single scattering approximation. Fourier transforms of EXAFS spectra were made after multiplication of the signal by a k^3 factor over a 2.8–14 $Å^{-1}$ Kaiser apodization window with τ = 2.5.[28]

S k-edge: XANES (*X-ray absorption near edge structure*) spectra were recorded at the SA32 beamline at LURE, using the SuperAco positron storage ring (800 MeV, ~173 mA). The beamline was equipped with a Ge (111) double crystal monochromator. The experiments were performed at room temperature in total yield electron mode. The energy was calibrated against the edge threshold position for ZnS (first intense peak on the first derivative dAbs *vs.* dE curve at 2473.0 eV). Two spectra were recorded from 2460 to 2560 eV with a step of 0.2 eV and 1 s of accumulation per point.

Scanning electron micrographs were recorded with a Cambridge Stereoscan 360 operating at 20 kV (Techinauv, A. S., Aubière, France).

Results and discussion

The process of adsorption

The orientation of the incorporated molecule is of great importance to better understand the formation of nanocomposites. Therefore the first steps of VBS and PSS interaction with the [Zn_2Al] LDH matrix are studied. As recently reported, VBS adsorption proceeds by a Langmuir mechanism, whereas PSS polymer adsorption adopts a Freundlich type behavior.[29] The study underlines the presence of a rapid mechanism for VBS adsorption, the molecule interacting strongly with [Zn_2Al] LDH substrate. The adsorption is accompanied by an intercalation process (see below). In contrast, PSS molecules meet strong competition to reach the substrate sites probably from the chlorine anions released during the adsorption reaction. XRD analysis is displayed in Fig. 1. For clarity, the 2θ domain is enlarged in the 2–15° range. For VBS interaction, in addition to the diffraction lines of Cl-[Zn_2Al] LDH, a diffraction peak at d = 18.2 Å appears on the X-ray diagrams. It is characteristic of the incorporation of VBS between LDH sheets with the

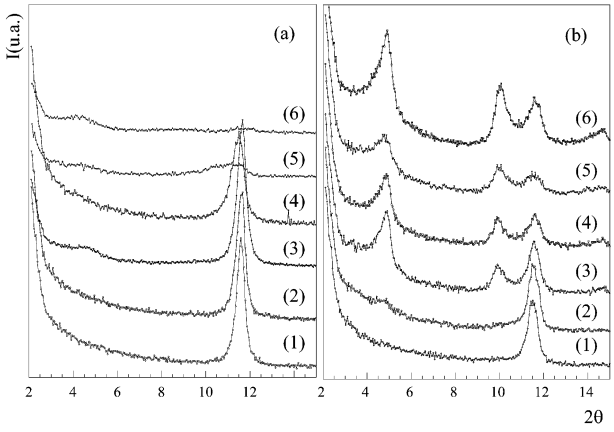

Fig. 1 XRD patterns of Cl-[Zn_2Al] phases adsorbed from a) PSS and b) VBS solution corresponding to a solution concentration of 1) C/40, 2) C/20, 3) C/10, 4) C/5, 5) C/4, and 6) C/2. C represents the LDH *anionic exchange capacity*.

Table 1 Chemical analysis of Cl-[Zn_2Al] and nanocomposite derivatives and the relative d-spacings

Sample	Chemical formulae	d-spacing/Å
Cl-[Zn_2Al]	$Zn_{0.67}Al_{0.33}(OH)_2Cl_{0.33}{\cdot}1.07\ H_2O$	7.8
VBS-[Zn_2Al]	$Zn_{0.67}Al_{0.33}(OH)_2(C_8H_7SO_3)_{0.32}{\cdot}0.72\ H_2O$	18.2
VBS-[Zn_2Al] 200 °C	$Zn_{0.67}Al_{0.33}(OH)_2(C_8H_7SO_3)_{0.33}{\cdot}0.55\ H_2O$	14.5
PSS-[Zn_2Al]	$Zn_{0.67}Al_{0.33}(OH)_2(C_8H_7SO_3)_{0.33}{\cdot}1.15\ H_2O$	19.3

presence of two layers of monomer.[20] No intercalation is observed for the PSS polymer, showing that the interaction proceeds only at the surface and edge of the crystallites. For higher polymer concentrations (Fig. 1a), the basal spacing disappears progressively and is absent for an amount of polymer equal to (LDH) AEC/5. It shows that the stacked layers are progressively dis-assembled until a quasi-complete delamination is reached, corresponding to a featureless XRD pattern. Similar results obtained by other procedures were ascribed to an exfoliation process.[30–32] In the present case, an increase in polymer concentration induces the formation of a PSS–LDH hybrid phase, showing that a solid is then recovered. Contrary to other guest molecules,[33,34] no staging is observed for VBS or PSS molecules.

Characterization of the hybrid phases

The molar ratio Zn : Al and the relative ion contents of the LDH materials are close to the expected values, indicating that the reaction was complete (Table 1). The exchange of chloride anions by VBS is also complete, this was confirmed by X-ray absorption spectroscopy used for sulfur XANES study, since a Cl *k*-edge is not observed. For the nanocomposite prepared by the *templating* method, the PSS amount is in agreement with what should theoretically be expected from the initial Zn : Al ratio.

[Zn_2Al] LDH material is well crystallized as observed by the X-ray diffraction pattern (Fig. 2a). Diffraction peaks are typical of the layered double hydroxide structure.[11] The reflections were indexed in a hexagonal lattice with a *R*-3*m* rhombohedral symmetry, commonly used for the description of the LDH structure. Miller indices are given in Fig. 2. Refined cell parameters are: $a = 3.07$ Å and $c = 23.37$ Å ($= 3*d_{003}$).

VBS incorporation between the layers of [Zn_2Al] LDH is confirmed by an increase of the basal spacing from 7.79 to 18.2 Å (Table 1). The value is the sum of the layer thickness, estimated to be 4.8 Å for the brucitic-like layers, and the interlayer distance. As before, it is in agreement with a VBS molecule lying perpendicular to the sheets and forming a bilayer in the interlamellar space.

The *as-made* PSS–LDH nanocomposite is poorly crystallized, as indicated in Fig. 3a. A subsequent hydrothermal treatment improves greatly the crystallinity of the sample

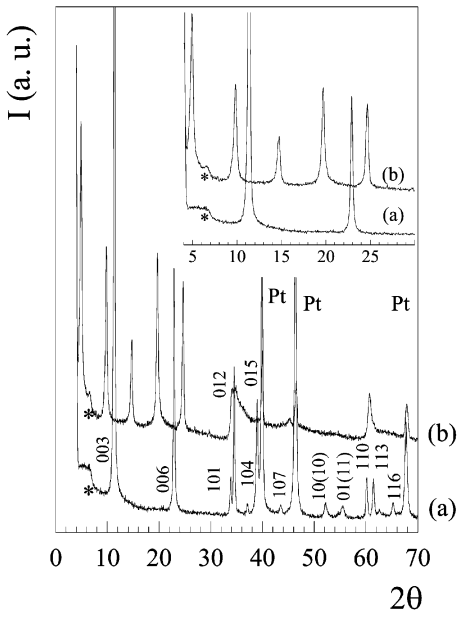

Fig. 2 XRD patterns of a) Cl-[Zn_2Al] LDH pristine material and b) VBS–[Zn_2Al] intercalation compound. The asterisk corresponds to the PSD response.

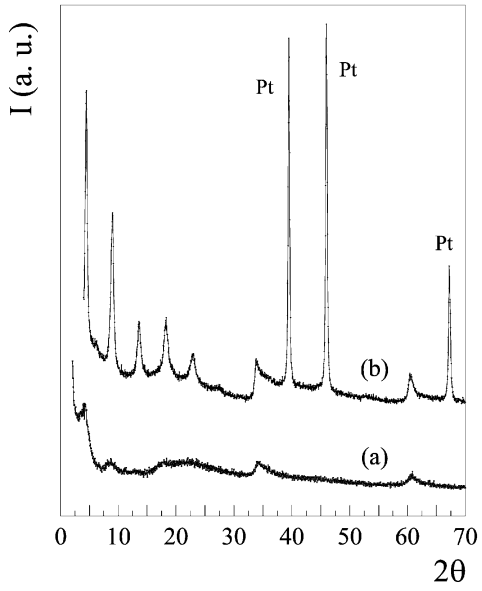

Fig. 3 XRD patterns of PSS–[Zn_2Al] nanocomposite a) as-prepared and b) after hydrothermal treatment.

(Fig. 3b). A basal spacing of $d = 19.3$ Å and the *in-plane* reflections (012) and (110) are observed, showing that the stacking of the layers was improved as well as the intralamellar organization.

The curing effect is studied at the local scale. The modulus of the Fourier transform of the PSS hybrid sample before and after the hydrothermal treatment is presented in Fig. 4. At first glance, the Zn *k*-edge spectra are keeping the expected features for both samples, *viz.* Zn–O and Zn–metal correlations. Refinements were in agreement with previous results.[35] The atomic contributions are, although not similar at longer range, as evidenced by an increase in intensity of P4 and P6 peaks (noted in Fig. 4) after the hydrothermal treatment. They arise from Zn–Me contributions at distances of 2*a* and 3*a*, respectively. They are enhanced by the so-called focusing (resp. superfocusing) effect,[35] coming from the linear situation between the atoms.[36]

It shows that the hydrothermal treatment stabilizes the sheets, leaving them more planar. The peak P3 corresponds to Zn–Me at av3, P5 for a distance of av7 is not observed.

To conclude, XAS study shows that the PSS–LDH nanocomposite exhibits a well-ordered structure, pointing

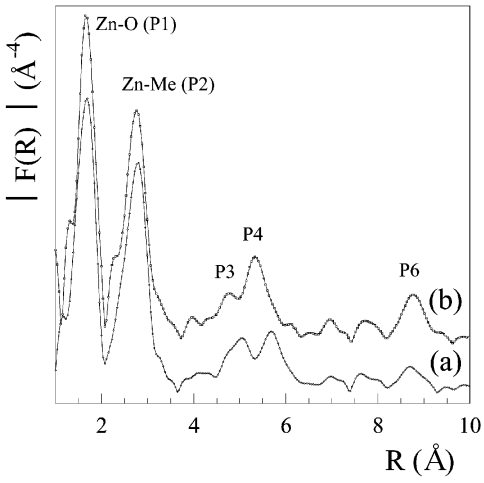

Fig. 4 Moduli of the Fourier transform at the Zn *k*-edge for the PSS–[Zn_2Al] nanocomposite a) before and b) after hydrothermal treatment. Distances are given without phase shift corrections.

out that the *templating* method is suitable but not sufficient to obtain a well-crystallized sample.

Interaction guest–host

Fig. 5 displays the ^{13}C CP-MAS spectra of a VBS molecule. The resonance peaks are assigned according to the literature:[37] C^1: 113.9 ppm, C^2: 137.4 ppm, C^3: 141.5 ppm, C^4: 125 ppm, and C^5: 143.8 ppm for $C^1H_2{=}C^2H\text{-}C^3(C_4{}^4H_4)C^5\text{-}SO_3(Na)$. When incorporated between $[Zn_2Al]$ LDH sheets, some resonance peaks are substantially shifted (Fig. 5b). It is associated with a shielding effect for C^2, C^3, and C^5 carbon atoms. These shifts may be explained from an electrostatic interaction between the SO_3 function with the LDH inner-surface, thus weakening the electrophilic character toward C^5. Such an effect propagates through the benzene backbone down to C^1 carbon atoms, which is shifted to down-field values.

It is interesting to note that a similar effect of the same amplitude is observed when VBS is incorporated into $[Zn_4Al]$ LDH, however, the layer charge density changes from 0.247 nm^2 per e^- to 0.413 nm^2 per e^- for $n = 2$ and 4 in $[Zn_nAl]$, respectively. One should expect a decrease of the interaction with a decrease of the layer charge.

To scrutinize such an effect on a long alkyl chain molecule, DBS–LDH hybrid samples were studied. The assignment of the resonance peak for a DBS molecule is reported in Fig. 6. After DBS incorporation, C^1 and C^3 carbon atoms are shifted from an initial position, equivalently for the LDH hosts, thus confirming our results for VBS. The resonance lines of C^n and C^4 carbon atoms remain at the same position, showing that the effect is not transmitted along the alkyl chain.

VBS was incorporated between the sheets of Cl-$[Ca_2Al]$ hydrocalumite affiliated to a LDH structure.[38] The shifts are of smaller amplitude.[39] It shows that the strength of interaction is independent of the layer charge density, but not of the LDH nature.

Similar results were obtained on silicate layers present in LDH.[40] From a ^{29}Si NMR study, the Q_3 resonance line, which gives the substitution of hydroxy groups by siloxane groups around a tetrahedral Si atom, $Si(OSi)_3OH$, are unmodified for $[Mg_nAl]$ LDH, $n = 2$ to 4.

In-situ polymerization

The XRD pattern of the VBS exchanged phase after thermal treatment at 180 °C is displayed in Fig. 7. The lamellar structure is contracted to 14.5 Å (Table 1). In comparison to a VBS intercalation compound pattern, the (00l) diffraction lines are much broader, whereas (012) and (110) lines are intact. It implies a slight decrease in the stacking sequence after the thermal treatment, although, leaving unmodified the intralamellar organization.

Similar contractions were observed for *in-situ* polymerization as exemplified in the case of α,β-aspartate (from 11.0 to 9.0 Å)[41] or acrylate (from 13.6 to 12.6 Å)[42,43] into hydrotalcite type compounds and ε-aminocaproic acid to nylon into a α-ZrP matrix (from 16.3 to 12.2 Å).[44]

The ^{13}C CP-MAS spectrum of the sample after thermal treatment at 180 °C was recorded (Fig. 8a). The resonance peaks of the material resemble that of PSS (Fig. 8d). C^1 contribution associated to the vinyl bond disappears and the formation of large humps located at ~40–50 ppm, characteristic of CH and CH_2 response, is observed. In the meantime, C^3 is shifted, as expected in the absence of a C=C bond.[37] It shows clearly that VBS molecules were polymerized in the interlayer space. Other temperatures for the heat treatment were applied.

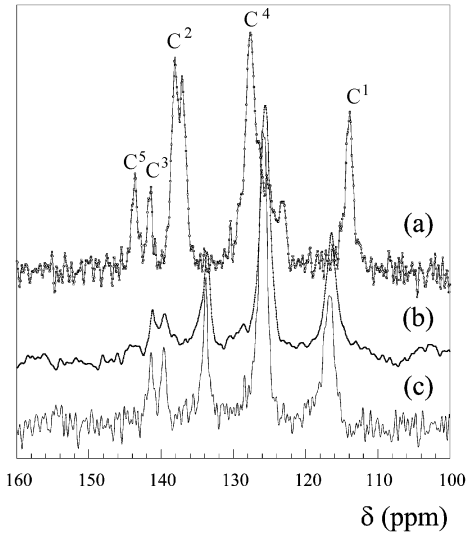

Fig. 5 ^{13}C CP-MAS spectra of a) VBS molecule, b) VBS–$[Zn_2Al]$ and c) VBS–$[Zn_4Al]$ intercalation compounds. See text for the assignments.

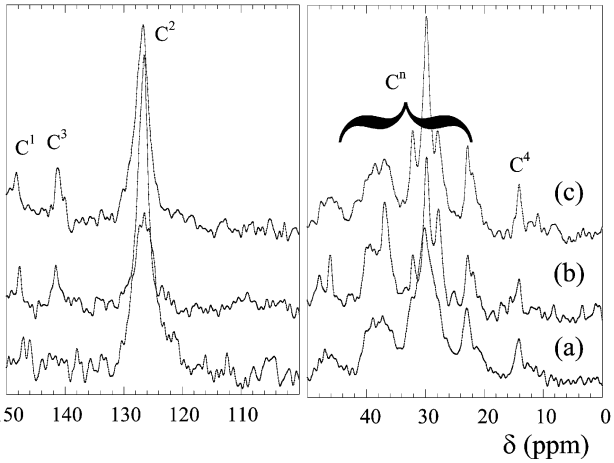

Fig. 6 ^{13}C CP-MAS spectra of a) DBS molecule, b) DBS–$[Zn_2Al]$ and c) DBS–$[Zn_4Al]$ intercalation compounds. The carbon atoms are referred to as $Na\text{-}O_3SC^1(C^2{}_4H_4)C^3(C^n{}_{11}H_{22})C^4H_3$.

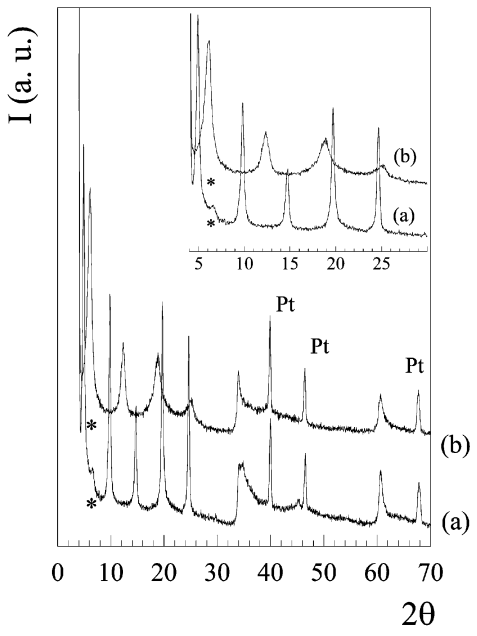

Fig. 7 XRD patterns of VBS–$[Zn_2Al]$ hybrid phase a) as-prepared and b) after thermal treatment at 180 °C. The asterisk corresponds to the PSD response.

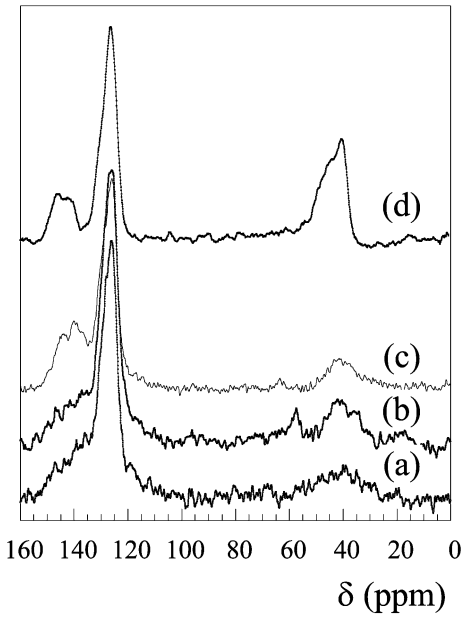

Fig. 8 ^{13}C CP-MAS spectra of VBS–[Zn_2Al] after treatment at a) 150 °C, b) 180 °C and c) 300 °C and d) PSS polymer.

^{13}C CP-MAS spectra of the samples present the same similarities. However, a more structured spectrum is obtained after 300 °C; C^5 and C^3 contributions at 143.7 and 139.7 ppm, respectively, are then observed.

A *d*-spacing of 14.5 Å supposes a highly confined arrangement of VBS in the interlamellar space. From the free space available for the polymer, we surmise that the *in-situ* polymerization gives rise to an atactic PSS. The intercalation of isotactic PSS results in a larger *d*-spacing stable up to 450 °C.[45]

To know if the lamellar contraction is accompanied with a grafting process, sulfur *K*-edge XANES of the samples was studied. The corresponding curves are displayed in Fig. 9. The spectrum of Na_2SO_4 is shown for comparison. The spectra are dominated by a single white-line feature reflecting the transitions 1s to *n*p and corresponding to localized, unfilled atomic or molecular states. The white line for the VBS–LDH phase is located at the same energy as a VBS molecule, *i.e.* 2481.6 eV. The energy is similar after thermal treatment at 180 °C. It shows that sulfur atoms are keeping the same coordination polyhedra up to 180 °C. At low temperature there is no indication of grafting contrary to other intercalation compound LDH systems.[46]

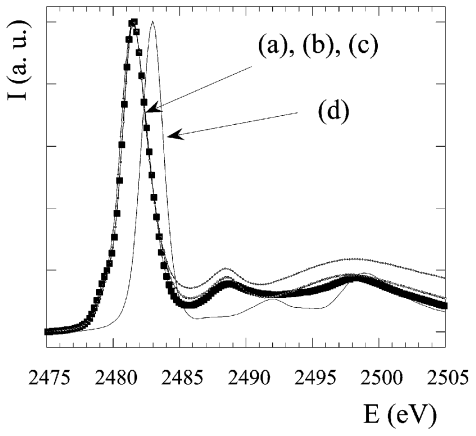

Fig. 9 XANES spectra at S *k*-edge of a) VBS molecule, VBS–[Zn_2Al] phase at b) room temperature and c) after 200 °C treatment and d) Na_2SO_4.

Largely employed for Al containing materials, ^{27}Al NMR is extremely sensitive in identifying the coordination state of aluminium atoms.[47–50] ^{27}Al spectra were recorded (Fig. 10). The materials were treated at 180 °C for 4 h, our standard procedure for the polymerization reaction. Even using a MAS condition at 10 kHz, the resonance lines are largely broadened by the quadropolar moment. It is known that the Al coordination site in Al containing LDH materials changes from *Oh* to *Td* with increasing temperature,[51] while the material sustains a lamellar organization.[52,53] Belloto *et al.* reported the conversion of *ca.* 10% of Al atoms in a [Mg_2Al] LDH matrix.[51]

Depending on the samples, two lines are observed, one at *ca.* 13 ppm, the other at 75 ppm (chemical shift not corrected). The former is assigned to Al atoms in an octahedral environment, the latter is attributed to Al tetrahedral sites. A conversion of Al coordination from *Oh* to *Td* is observed for Cl-[Zn_2Al] pristine material, it is attenuated for a PSS–LDH nanocomposite and absent for VBS hybrid material. The *in-situ* polymerization precludes the change of coordination for Al cations. It may be explained by either an anchoring of VBS molecules on the inner-surface of the LDH or by a steric restriction with the presence of polymer strongly confined, thus hindering the presence of AlO_4 structural units. The S *k*-edge analysis dismissed the first possibility.

Textural properties

As observed for other organoceramics such as PVA–hydrocalumite, the morphology of the nanocomposite is different from the host material.[54] After VBS exchange reaction, the sand-rose morphology of the pristine material is lost to the profit of a crumpled aspect (Fig. 11). The size of the platelets is substantially reduced for the intercalation compound. This was evidenced by an increase in the full width at middle height (F. W. M. H) of the diffraction peaks. The treatment at 180 °C does not change significantly the morphology of the sample. The morphology of the PSS–LDH nanocomposite differs with the presence of large chunks. It is related to the synthesis pathway, with the LDH crystal being *self-assembled* on the polymer.

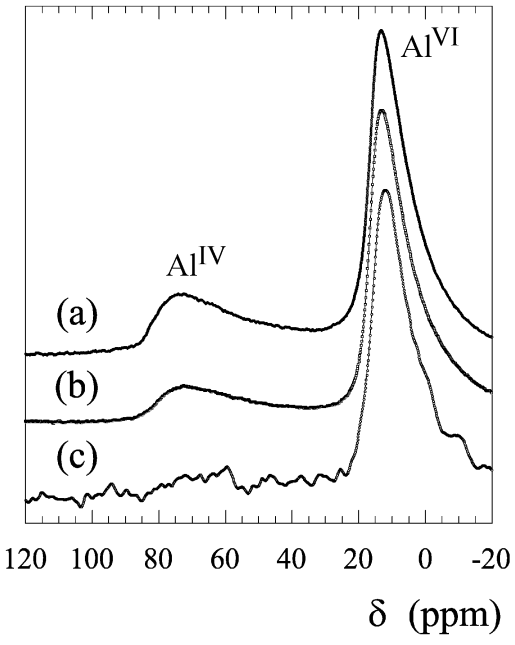

Fig. 10 ^{27}Al MAS spectra of samples after a 180 °C treatment a) Cl-[Zn_2Al] LDH, b) VBS–[Zn_2Al] and c) PSS–[Zn_2Al] nanocomposite. Chemical shifts are not corrected from the 2nd effect of the quadrupolar interaction.

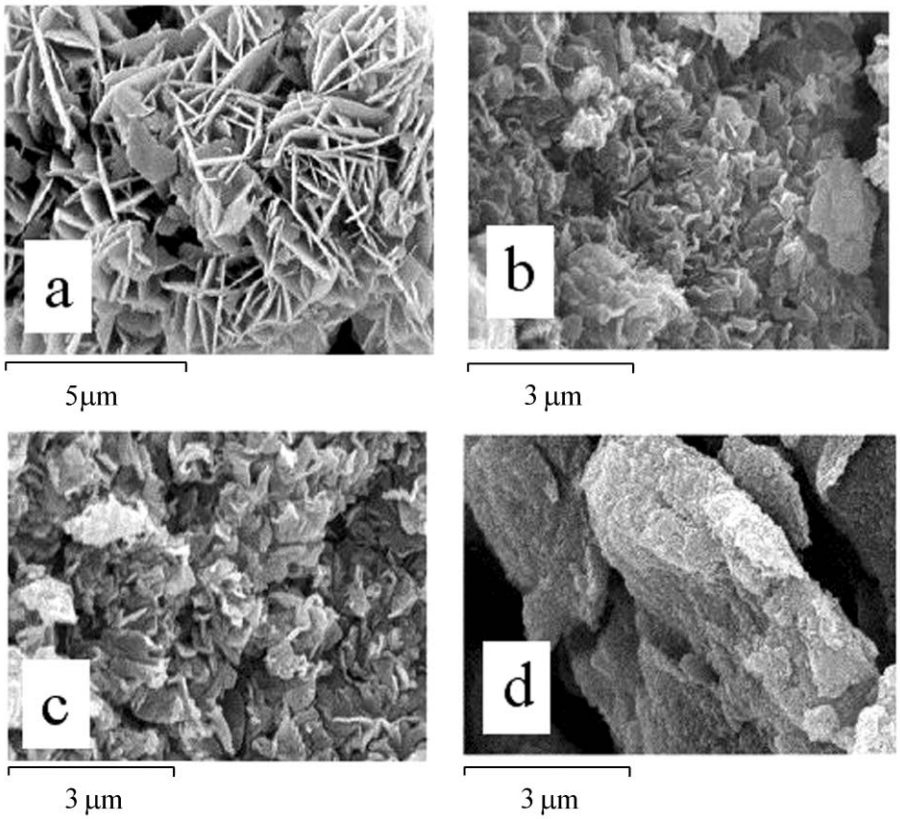

Fig. 11 SEM pictures of a) Cl-[Zn_2Al] LDH material, VBS–[Zn_2Al] phase at b) room temperature and c) after *in-situ* polymerization and d) PSS–[Zn_2Al] nanocomposite.

Conditions for the *in-situ* polymerization

We were unsuccessful at polymerizing a VBS monomer between [Zn_nAl] LDH sheets, $n = 3$ and 4, even using longer times for the thermal treatment. C^1 contribution remains present (Fig. 12). It shows that the layer charge density of the host structure is an important factor for the polymerization process to be achieved.

Considering the projected surface area of the SO_3 group of 0.22 nm^2 per e^-, we believe that the monomer molecules are situated too far from each other for the polymerization to proceed for [Zn_nAl] LDH, $n = 3$ and 4, whereas it suits well the [Zn_2Al] host structure. The situation points out the matching between a guest molecule and a host structure, as evidenced for other organic–inorganic systems.[55]

The confinement into LDH interlamellar space is necessary to complete the polymerization, since the reaction is not complete for VBS molecules (Fig. 12).

To know if the oxygen molecules may influence the polymerization reaction as observed for aniline sulfonate monomer,[56] the thermal treatment was performed under nitrogen atmosphere. Treatment for 4 h is not sufficient, longer exposure times give rise to a total polymerization.

Generalization

The reaction was extended to another LDH material, Cl-[Mg_2Al]. As for [Zn_2Al] LDH, the hybrid phase exhibits a complete exchange of the chlorine anions by VBS molecules.

In-situ polymerization was reached for VBS–[Mg_2Al] LDH nanocomposite using a thermal treatment at 180 °C for 4 h (Fig. 13). The C^1 resonance peak disappears from the ^{13}C CP-MAS spectrum, the features reflect the presence of PSS. It shows the possible extension of the reaction to other LDH materials.

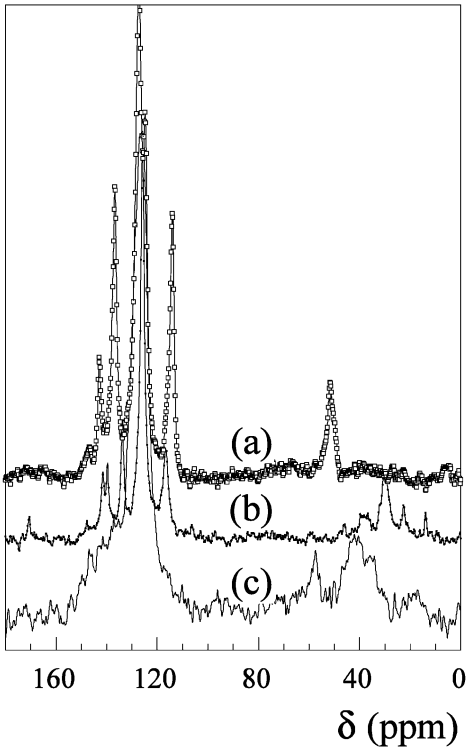

Fig. 12 ^{13}C CP-MAS spectra of samples after treatment at 200 °C for 6 h a) VBS molecule, b) VBS–[Zn_3Al] intercalation compound. The spectrum of Fig. 8b is displayed in comparison in c).

Conclusion

We demonstrate that *in-situ* polymerization of a VBS molecule may be achieved between LDH sheets *via* soft thermal

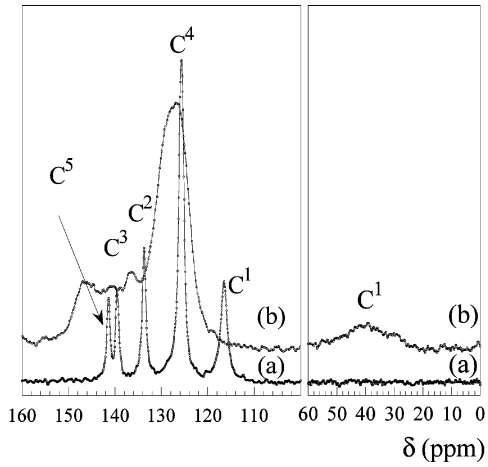

Fig. 13 ^{13}C CP-MAS spectra of VBS–[Mg_2Al] sample at a) room temperature and b) after treatment at 180 °C. Same assignments as for Fig. 5.

treatment. No grafting is evidenced during the polymerization reaction. The monomer is found to interact strongly with the inner-surface of the LDH. The driving force is the mutual attraction between the positive charge of the layer and the sulfonate group. It shows that a matching between the guest molecule and the layer charge is required for the polymerisation reaction to occur.

The two procedures, *i.e.* the *templating* method and *in-situ* polymerization, give different nanocomposites in term of crystallinity and structural stability. PSS adsorption induces the delamination of Cl-[Zn_2Al], and opens new possibilities for LDH dispersion.

Finally, polymerization of VBS is generalized to other LDH materials.

Acknowledgements

The authors are grateful to Joël Cellier (LMI) for his assistance and to Anne-Marie Gélinaud for the SEM pictures. We also thank Dr Anne-Marie Flank and Valérie Briois for their help in acquiring XAS spectra, and LURE for the use of the facilities.

References

1 J. Wang, J. Merino, P. Aranda, J.-C. Galvan and E. Ruiz-Hitzky, *J. Mater. Chem.*, 1999, **9**, 161.
2 C. O. Oriakhi, *J. Chem. Ed.*, 2000, **77**, 1138.
3 P. Gomez-Romero, *Adv. Mater.*, 2001, **13**, 163.
4 F. Leroux and J.-P. Besse, *Chem. Mater.*, 2001, **13**, 3507.
5 J. Bujdak, E. Hackett and E. Giannelis, *Chem. Mater.*, 2000, **12**, 2168.
6 Z. Wang, T. Lan and T. J. Pinnavaia, *Chem. Mater.*, 1996, **8**, 2200.
7 H. Shi, T. Lan and T. J. Pinnavaia, *Chem. Mater.*, 1996, **8**, 1584.
8 E. Ruiz-Hitzky and P. Aranda, *Adv. Mater.*, 1990, **2**, 545.
9 J. W. Gilman, C. L. Jackson, A. B. Morgan Jr., R. Harris, E. Manias, E. P. Giannelis, M. Wuthenow, D. Hilton and S. H Philips, *Chem. Mater.*, 2000, **12**, 1866.
10 J. Zhu, F. M. Uhl, A. B. Morgan and C. A. Wilkie, *Chem. Mater.*, 2001, **13**, 4649.
11 W. Hofmeister and H. von Platen, *Cryst. Rev.*, 1992, **3**, 3.
12 G. W. Brindley and S. Kikkawa, *Am. Mineral.*, 1979, **64**, 836.
13 A. J. Jacobson, *Mater. Science Forum*, 1994, **152-153**, 1.
14 M. G. Kanatzidis, C.-G. Wu, H. O. Marcy, D. C. DeGroot and C. R. Kannewurf, *Chem. Mater.*, 1990, **2**, 222.
15 H.-J. Nam, H. Kim, S. H. Chang, S.-G. Kang and S.-H. Byeon, *Solid State Ionics*, 1999, **120**, 189.
16 M. G. Kanatzidis, L. M. Tonge and T. J. Marks, *J. Am. Chem. Soc.*, 1987, **109**, 3797.
17 L. Wang, P. Brazis, M. Rocci, C. R. Kannewurf and M. G. Kanatzidis, *Chem. Mater.*, 1998, **10**, 3298.
18 T. A. Kerr, H. Wu and L. F. Nazar, *Chem. Mater.*, 1996, **8**, 2005.
19 P. Liu, K. Gong, P. Xiao and M. Xiao, *J. Mater. Chem.*, 2000, **10**, 933.
20 C. O. Oriakhi, I. V. Farr and M. M. Lerner, *J. Mater. Chem.*, 1996, **6**, 103.
21 P. B. Messersmith and S. I. Stupp, *J. Mater. Res.*, 1992, **7**, 2599.
22 L. Wang, J. Schindler, C. R. Kannewurf and M. G. Kanatzidis, *J. Mater. Chem.*, 1997, **7**, 1277.
23 H.-L. Tsai, J. L. Schindler, C. R. Kannewurf and M. G. Kanatzidis, *Chem. Mater.*, 1997, **9**, 875.
24 C. O. Oriakhi, I. V. Farr and M. M. Lerner, *Clays Clay Miner.*, 1997, **45**, 194.
25 O. Y. Posudievsky, S. A. Biskulova and V. D. Pokhodenko, *J. Mater. Chem.*, 2002, **12**, 1446.
26 S. Miyata, *Clays Clay Miner.*, 1980, **28**, 50.
27 G. Engelhardt and D. Michel, In *High-Resolution Solid State NMR of Silicates and Zeolites*, Wiley, New York, 1987.
28 A. Michalowicz, Round Midnight, EXAFS Signal Treatment and Refinement Programs, LURE, Orsay, France. Programs available on LURE Web site; http://www.LURE.fr.
29 M. El Moujahid, J. Inacio, J.-P. Besse and F. Leroux, *Microporous Macroporous Mater.*, in press.
30 M. Adachi-Pagano, C. Forano and J.-P. Besse, *Chem. Commun.*, 2000, 91.
31 T. Hibino and W. Jones, *J. Mater. Chem.*, 2001, **11**, 1321.
32 F. Leroux, M. Adachi-Pagano, M. Intissar, S. Chauvière, C. Forano and J.-P. Besse, *J. Mater. Chem.*, 2001, **11**, 105.
33 N. Iyi, K. Kurashima and T. Fujita, *Chem. Mater.*, 2002, **14**, 583.
34 L. Lei, R. P. Vijayan and D. O'Hare, *J. Mater. Chem.*, 2001, **11**, 3276.
35 H. Roussel, V. Briois, E. Elkaïm, A. de Roy and J.-P. Besse, *J. Phys. Chem.*, 2000, **104**, 5915.
36 N. Alberding and E. D. Crozier, *Phys. Rev. B*, 1983, **27**, 3374.
37 G. Geismar, J. Lewandowski and E. de Boer, *Chemiker Zeitung*, 1991, **115**, 335.
38 C. E. Tilley, H. D. Megaw and M. H. Hey, *Min. Mag.*, 1934, **23**, 607.
39 L. Vieille, C. Taviot-Guého and F. Leroux, unpublished results.
40 S. K. Yun, V. R. L. Constantino and T. J. Pinnavaia, *Clays Clay Miner.*, 1995, **43**, 503.
41 N. T. Whilton, P. J. Vickers and S. Mann, *J. Mater. Chem.*, 1997, **7**, 1623.
42 M. Tanaka, I. Y. Park, K. Kuroda and C. Kato, *Bull. Chem. Soc. Jpn.*, 1989, **62**, 3442.
43 S. Rey, J. Mérida-Robles, K.-S. Han, L. Guerlou-Demourgues, C. Delmas and E. Duguet, *Polym. Int.*, 1999, **48**, 277.
44 Y. Ding, D. J. Jones, P. Maireless-Torres and J. Rozière, *Chem. Mater.*, 1995, **7**, 562.
45 M. Moujahid El and F. Leroux, unpublished results.
46 V. Prevot, C. Forano and J.-P. Besse, *Applied Clay Sci.*, 2001, **18**, 3.
47 J. Rocha and J. Klinowski, *Angew. Chem.*, 1990, **29**, 553.
48 Z. Luan, M. Hartmann, D. Zhao, W. Zhou and L. Kevan, *Chem. Mater.*, 1999, **11**, 1621.
49 S. M. Bradley and J. V. Hanna, *J. Am. Chem. Soc.*, 1994, **116**, 7771.
50 K. Kosuge and P. S. Singh, *Chem. Mater.*, 2001, **13**, 2476.
51 M. Belloto, B. Rebours, O. Clause, J. Lynch, D. Bazin and E. Elkaim, *J. Phys. Chem.*, 1996, **100**, 8535.
52 J. Rocha, M. del Arco, V. Rives and M. A. Ulibarri, *J. Mater. Chem.*, 1999, **9**, 2499.
53 F. Rey, V. Fornes and J. M. Rojo, *J. Chem. Soc., Faraday Trans.*, 1992, **88**, 2233.
54 P. B. Messersmith and S. I. Stupp, *Chem. Mater.*, 1995, **7**, 454.
55 C. G. Wu, D. C. DeGroot, H. O. Marcy, J. L. Schindler, C. R. Kannewurf, T. Bakas, V. Papaefthymiou, W. Hirpo, J. P. Yesinowski, Y. J. Liu and M. G. Kanatzidis, *J. Am. Chem. Soc.*, 1995, **117**, 9229.
56 M. El Moujahid, M. Dubois, J.-P. Besse and F. Leroux, *Chem. Mater.*, 2002, **14**, 3799.